

## Projected Effects of Climate Change on Urban Ozone Air Quality by Using Artificial Neural Network Approach; Case Study: Tehran Metropolitan Area, Iran

Mosadegh, E.<sup>1</sup>  | Babaeian, I.<sup>2</sup>  | Ashrafi, Kh.<sup>3</sup>  | Shafiepour Motlagh, M.<sup>3</sup> 

1. Atmospheric Sciences Graduate Program, University of Nevada, Reno, USA.
2. Climate Research Institute, Atmospheric Science and Meteorological Research Center, Mashhad, Iran.
3. Department of Environmental Engineering, Faculty of Environment, University of Tehran, Tehran, Iran.

**Corresponding Author E-mail:** [emosadegh@nevada.unr.edu](mailto:emosadegh@nevada.unr.edu)

(Received: 6 June 2022, Revised: 4 Jan 2023, Accepted: 2 May 2023, Published online: 20 Feb 2024)

### Abstract

We developed an artificial neural network as an air quality model and estimated the scope of the climate change impact on future (until 2064) summertime trends of hourly ozone concentrations at an urban air quality station in Tehran, Iran. Our developed scenarios assume that present-time emissions conditions of ozone precursors will remain constant in the future. Therefore, only the climate change impact on future ozone concentrations is investigated in this study. General Circulation Model (GCM) projections indicate more favorable climate conditions for ozone formation over the study area in the future: the surface temperature increases over all months of the year, solar radiation increases, and precipitation decreases in future summers, and summertime daily maximum temperature increases about 1.2°C to 3°C until 2064. In the scenario based on present-time ozone conditions in the 2012 summer without any exceedances, the summertime exceedance days of the 8-hr ozone standard are projected to increase in the future by about 4.2 days in the short term and about 12.3 days in the mid-term. Similarly, in the scenario based on present-time ozone conditions in the 2010 summer with 58 days of exceedance from the 8-hr ozone standard, exceedances are projected to increase by about 4.5 days in the short term and about 14.1 days in the mid-term. Moreover, the number of Unhealthy and Very Unhealthy days in the 8-hr Air Quality Index (AQI) is also projected to increase based on pollution scenarios of both summers.

**Keywords:** Ozone, Climate change, Air quality modeling, Artificial neural networks, Tehran.

### 1. Introduction

Intergovernmental Panel on Climate Change (IPCC) projections indicate that climate change may influence future air quality, and the magnitude of the impact varies from one region to another (IPCC, 2007). One challenge associated with air quality studies is to quantify this influence on air pollutants such as ozone and particulate matter, which are sensitive to climate changes (Jacob and Winner, 2009). Surface ozone, which is one of the most important air pollutants, degrades public health by damaging the respiratory system. It is a secondary pollutant that means it is not emitted from a particular source but is produced through complex photochemical reactions among its biogenic and anthropogenic precursors such as Nitrogen Oxides (NO<sub>x</sub>), Non-Methane Volatile Organic Compounds (NMVOC), Carbon Monoxide (CO) and Methane (CH<sub>4</sub>) in the presence of high temperature and abundant

sunlight (Jacob and Winner, 2009; Seinfeld and Pandis, 2006; Steiner et al., 2006). NO<sub>x</sub> and CO come from combustion sources, but NMVOC and CH<sub>4</sub> have several natural and anthropogenic sources (Guenther et al., 2000; Sillman, 1999). Therefore, due to its photochemical nature, ozone concentrations generally peak during summer when meteorological conditions are often favorable for its formation. Ozone has an atmospheric lifetime of about a few days in the boundary layer with global sinks of dry deposition and photolysis in the presence of water vapor (Jacob and Winner, 2009). This oxidant pollutant irritates the pulmonary system and decreases lung function. Ozone is believed to be associated with premature mortality and exposure to its elevated concentrations irritates people who have respiratory diseases such as asthma and pneumonia (Bell et al., 2007; Ebi and McGregor, 2008; Gryparis et

**Cite this article:** Mosadegh, E., Babaeian, I., Ashrafi, Kh., & Shafiepour Motlagh, M. (2024). Projected Effects of Climate Change on Urban Ozone Air Quality by Using Artificial Neural Network Approach; Case Study: Tehran Metropolitan Area, Iran. *Journal of the Earth and Space Physics*, 49(4), 121- 141. DOI: <http://doi.org/10.22059/jesphys.2023.342978.1007432>

**E-mail:** (2) [i.babaeian@gmail.com](mailto:i.babaeian@gmail.com) (2) [khashrafi@ut.ac.ir](mailto:khashrafi@ut.ac.ir) | [shafiepourm@yahoo.com](mailto:shafiepourm@yahoo.com)



Publisher: University of Tehran Press.  
DOI: <http://doi.org/10.22059/jesphys.2023.342978.1007432>

Print ISSN: 2538-371X  
Online ISSN: 2538-3906

al., 2004).

Meteorological parameters play an important role in ozone production. Temperature, solar radiation, atmospheric moisture, wind, mixing height, precipitation and cloud cover are identified to be correlated with ozone (Camalier et al., 2007; Dawson et al., 2007; Leibensperger et al., 2008; Mott et al., 2005; Ordóñez et al., 2005). Among these variables, ozone is highly sensitive to temperature (Cox and Chu, 1996; Dawson et al., 2007; Sillman and Samson, 1995). The emission of biogenic Volatile Organic Compounds (VOCs), which is a temperature-dependent process can produce a considerable amount of ozone in high temperatures (Fuentes et al., 2000; Lee and Wang, 2006; Narumi et al., 2009). However, in addition to temperature, solar radiation is also necessary for the photochemical process of ozone formation in the atmosphere. The correlation between these variables is significant especially in summers when high radiation and temperature result in summer high ozone concentrations (Ordóñez et al., 2005).

There are two major sources of uncertainty in projections of the impact of climate change on future ozone formation: estimating the future emissions of ozone precursors and projecting the meteorological factors that strongly influence air quality (Dawson et al., 2007; Ebi and McGregor, 2008; Steiner et al., 2006). Studies that have investigated the influence of projected changes in climate variables on future ozone concentrations by assuming no changes in the emissions of ozone precursors (Dawson et al., 2009; Liao et al., 2006; Murazaki and Hess, 2006; Racherla and Adams, 2006) indicate that the projected changes in climate variables are expected to increase future ozone concentration levels over and near polluted regions. The extent of this increase, although varying in different regions, highlights the role of future meteorological conditions in ozone production and suggests that future meteorological parameters will shift toward more favorable conditions for ozone formation (Murazaki and Hess, 2006). We can perform sensitivity studies to evaluate how much changes in future emissions and climate can affect future ozone production (Dawson et al., 2007; Millstein and Harley, 2009; Orru et al., 2013; Steiner et al., 2006).

Steiner et al. (2006) found that combined climate perturbations (such as increases in temperature and water vapor together with the temperature-induced increase in biogenic VOC emissions) yield increased peak ozone concentrations. Their results indicate that the sensitivity of ozone to climate change is regionally different and the sensitive regions may experience more exceedances despite the present emission reduction policies; therefore, additional control on pollution emission reductions will be needed.

To study the impact of climate change on future ozone air quality both statistical and dynamical approaches can be used (Wise, 2009). Dynamical models have distinct advantages over statistical approaches. However, some benefits of statistical models cannot be ignored. Statistical models are widely known for their computationally inexpensive cost and capability of rapid climate change impact assessment by employing various climate models and scenarios. For instance, Varotsos et al. (2013) developed a statistical model between daily maximum temperature and hourly ozone concentrations over Europe for the periods of 2021–2050 and 2071–2100 to investigate the impact of climate change on the number of days with ozone exceedances of 60 ppb. They observed that higher daily temperatures due to the climate change will result in considerable increases in ozone exceedance days in the future. Also, one can use a statistical technique to downscale the General Circulation Model (GCM) data and model the relationship between observed ozone concentrations and meteorological variables to project the potential impact of future meteorology on ozone exceedances of 84 ppb (Holloway et al., 2008). Due to the coarse spatial resolution of GCM models, some of the small-scale but important processes are not captured in GCM simulations (Holloway et al., 2008). Also, dynamical models that are developed based on current physical parameterizations may not perfectly simulate future changes in climate variables. For instance, Lynn et al. (2004) showed that for climate change simulations to provide a realistic estimate of temperature changes, models should correctly simulate the diurnal precipitation over the study region.

Climate change projections (IPCC, 2021) indicate that projected changes in climate

variables such as precipitation and temperature (Mosadegh and Babaeian, 2022a) will impact different components of the climate system with different magnitude and confidence and in all regions of the world (Mejia et al., 2018; Mosadegh et al., 2018; Mosadegh and Nolin, 2020; Mosadegh and Nolin, 2022). Several studies have addressed the issue of air quality in Tehran (Arhami et al., 2013; Atash, 2007; Hosseinpour et al., 2005; Hoveidi et al., 2013). However, a few studies have investigated the uncertainty of those climate projections over the 21<sup>st</sup> century (Mosadegh and Babaeian, 2022b), and the extent that the projected climate variables can affect air pollution in Tehran (Mosadegh, 2013). The present study is the first attempt to evaluate the regional impact of climate change on air quality in Iran. This study aims to develop and apply a statistical approach to investigate the impact of climate change on future ozone air quality on a local scale in an urban environment. In this study, an artificial neural network was used as a predictive tool that is capable of capturing nonlinearities in atmospheric processes such as ozone formations (Comrie, 1997; Gardner and Dorling, 1998). The projected ozone concentrations were analyzed based on exceedances of ozone air quality standards and health-related air quality indices. To simplify the impact assessment process, only climate variables of solar radiation and temperature together with pollutants of Nitrogen Monoxide (NO) and Nitrogen Dioxide (NO<sub>2</sub>) were considered in the simulation process. In this study, the relationship between ozone and local meteorology was partially accounted for by considering hourly temperature and solar radiation values in the development process of the Artificial Neural Network as the air quality forecast model (AQFM). Emissions of ozone precursors were also taken into account but were considered constant based on current conditions. Therefore, only the impact of climate change was investigated on future ozone concentrations in Tehran.

## 2. Methods

This study comprises a few major steps: in the first step, we downscaled GCM data under different emission scenarios. In the second step, we downscaled the daily climate

variables from the previous step from the daily scale to the sub-daily (hourly) scale. In the third step, we developed input scenarios and developed an artificial neural network as the AQFM, and in the final step, we assessed the impact of climate change on future ozone air quality. These steps are described in detail in the next sections.

### 2-1. Case study and data

With a population of over 10 million people and with an area of approximately 570 square kilometers, Tehran is the capital and the largest city of Iran. Tehran is surrounded by mountains to the north and the east, and the wind directions are from the west and the south. Tehran suffers from serious air pollution problems. Motor vehicles are considered one of the major sources of air pollution in the Tehran metropolitan area due to their high emission of major pollutants such as CO, PM<sub>10</sub>, and NO<sub>2</sub> (Halek et al., 2004). In Tehran, air pollution concentrations are monitored by the Air Quality Control Company (AQCC) and the Department of Environment (DOE) in several air quality stations. In this study, the air quality data were obtained from the AQCC Golbarg air quality monitoring station east of Tehran at 35° 43' N and 51° 30' E. To develop and evaluate our AQFM, hourly monitored NO, NO<sub>2</sub>, ozone, solar radiation, and temperature collected at this station during 2009–2012 were used. Meteorological data were obtained from the Dushan Tappeh station, the nearest synoptic station located at 35° 42' N and 51° 20' E with a height of 1209 m above sea level. From this station, daily minimum temperature, daily maximum temperature, total precipitation, and total sunshine hours during 1972–2009 (baseline period) were used to calibrate the Long Ashton Research Stochastic Weather Generator (LARS-WG) statistical downscaling model.

### 2-2. Statistical downscaling with LARS-WG

Different dynamic and statistical models have been developed to downscale the GCM outputs (Wilby et al., 2004). Stochastic weather generators (WG) are one of the statistical downscaling tools, which generate daily time series of climate variables (Semenov, 2007; Wilks and Wilby, 1999). In this study, Long Ashton Research Stochastic

Weather Generator (LARS-WG) is employed to downscale the GCM projections and to estimate future changes in temperatures, solar radiation and precipitation over the study area. LARS-WG (Semenov and Barrow, 2002) is a stochastic weather generator (WG). The model takes observed daily minimum temperature, maximum temperature, total precipitation and total sunshine hours as its inputs and generates synthetic daily time series at any local scale. LARS-WG generates local-scale climate change scenarios for a given site by adjusting baseline parameters, calculated from baseline observed weather at the site, with projected GCM  $\Delta$ -changes, calculated based on an emission scenario called Special Report on Emissions Scenarios (SRES) and a future climate period, for each climatic variable (Semenov and Stratonovitch, 2010). More details about the application of the LARS-WG model can be found in Mosadegh and Babaeian (2022a, 2022b). The ability of the LARS-WG to simulate the baseline climate variables at the given site was evaluated by calculating the Pearson correlation coefficient (R) and error indices such as mean bias error (MBE), mean absolute error (MAE) and root mean square error (RMSE).

### 2-3. The AQFM

With recent advances in deep learning for pattern recognition, the performance of these networks for the task of prediction in different fields of environmental science has progressed even with a small amount of training data (Alibak et al., 2022; Nejatishahidin et al., 2022). The application of artificial neural networks (ANN), especially multilayer perceptions (MLP) in the field of air quality has been evaluated in many studies (Chaloulakou et al., 2003; Comrie, 1997; Niska et al., 2004; Schlink et al., 2003; Sousa et al., 2007). Application of the neural networks in forecasting ozone concentrations has been compared with other statistical tools such as multivariate linear regression models, and the results indicate that the ANNs, especially the MLP neural network, has a better performance over other techniques in modeling the ozone nonlinear associations (Gardner and Dorling, 1998). Furthermore, it can model highly nonlinear processes by its activation and transfer functions in the hidden layers (Rahnama and

Noury, 2008). These features make MLP a suitable tool for modeling complex, nonlinear phenomena such as ozone formation in the atmosphere.

In this study, a four-layer MLP (ANN) with a 4-10-10-1 (4 inputs with 1 output) network structure was developed and used as our AQFM. Tangent sigmoid transfer functions (*tansig*) were used in the hidden layers, but a linear transfer function (*purlin*) was used in the output layer. For training the network, the Levenberg-Marquardt back-propagation learning rule (*trainlm*) was used due to its fast speed and accuracy in training the system (Beale et al., 2012).

To determine the model inputs, we considered effective variables in ozone production (Ordóñez et al., 2005) and the limited number of available monitored variables at the Golbarg air quality control station. Finally, we selected NO, NO<sub>2</sub> and ozone as the air quality variables, and temperature and solar radiation as climate variables to develop the AQFM. It is noteworthy that the selected variables were monitored at *Golbarg* air quality monitoring stations during the summers (June, July and August, hereafter JJA) of 2009–2012.

To develop the training dataset for our ANN-based model, we first performed quality control on the training dataset. To control the quality of the training data, we followed the following steps. For any missing values in a parameter within a day, we first checked whether the missing values spanned one hour or more than one hour. If the missing values were for one hour, we computed the average of the observations before and after that time and filled in the missing values with the average value. However, if the missing values spanned more than one hour, we removed the rows with missing data from the training dataset. If any data sample contained negative values, the entire data sample was removed from the training dataset. Moreover, we removed the whole data samples for a variable if it had constant values in a day.

The selection of the data samples for developing the training dataset was limited to an interval of 8 am to 7 pm, which is the most effective period of ozone production during the day. Finally, about 4000 hourly data samples were obtained for the summers (JJA) of 2009 to 2012 to develop the forecast model. The training data set was shuffled

randomly to scatter maximum and minimum values evenly over the entire training data set. Then, data samples were divided into three subsets of training, test, and validation sets with 60-20-20 percent of the data set, respectively. Since the input and target variables did not have a uniform range of values, a normalization method was used to scale the input variables to have a certain range. In this study, normalization of the variables was performed by the *mapminmax* function in MATLAB to scale the data to the range [-1, 1] before fitting data to the main network. To achieve the best relationship between input variables and output target (ozone), different network architectures were examined. Finally, the network structure with the smaller error and the higher correlation was selected as the optimal predictive model.

To evaluate the performance of the AQFM, we calculated the correlation coefficient (R) and statistical parameters such as mean bias error (MBE), mean absolute error (MAE), and root mean square error (RMSE). After ensuring the accuracy of the simulations of the developed model to reproduce hourly ozone concentrations with high correlation coefficient and low error indices compared to similar studies (Arhami et al., 2013; Comrie, 1997; Sousa et al., 2007), the performance of the forecast model was assessed based on two performance indices. In this study, the prediction of exceedances of desired ozone air quality concentration thresholds was more important than predicting the exact ozone concentration values. Therefore, we developed two metrics to define capturing the occasions in which the ozone concentrations exceed a desired ozone air quality threshold. The two performance indices of PI1 and PI2 are described as follows:

PI1: The percentage of correctly identified occasions in which ozone concentrations exceeded a desired threshold.

PI2: The percentage of incorrectly identified occasions.

PI1 indicates the forecasting accuracy of the predicting model at each concentration threshold. This index represents the percentage of the cases that both monitored values and corresponding simulated values that exceed a desired concentration threshold and consequently, the model is successful in predicting the exceedance. PI2 indicates the

overestimation error of the model at each concentration threshold. This index represents the percentage of cases in that observations do not exceed the desired concentration threshold, but the model incorrectly indicates that the corresponding simulated values exceed the desired threshold.

To assess the accuracy of the AQFM in simulating the exceedances, several important ozone concentration thresholds were considered from various EPA ozone air quality standards and indices. The test data set of the model was examined to assess the accuracy of the model in predicting the exceedances. The investigated EPA thresholds are significant levels of ozone concentrations in 1-hr ozone air quality standard and air quality index (AQI). Exceeding these threshold concentrations results in the occurrence of an *Unhealthy* day (ozone concentration above 125 ppb) and a *Very Unhealthy* day (ozone concentrations above 205 ppb) from an AQI perspective, and the occurrence of a polluted day (ozone concentrations above 120 ppb) from 1-hr ozone standard perspective. In addition to mentioned thresholds, the accuracy of the forecast model in predicting exceedances of other concentration thresholds (25 ppb and 45 ppb) was also evaluated to enable us to compare the performance of the developed model with similar studies.

#### 2-4. Temporal (sub-daily) downscaling

LARS-WG generates minimum and maximum temperature values every single day. Solar radiation is also generated in  $Mj/m^2.day$  and represents the total solar radiation reaching the earth's surface in a single day. However, the AQFM was developed based on hourly (sub-daily) variables and received hourly temperature and radiation values as its inputs. For the LARS-WG output to match the AQFM inputs on an hourly (sub-daily) scale, we developed the diurnal distribution equations of the temperature and solar radiation at the given site to calculate the diurnal distribution of these variables. Also, several papers indicate that the ozone exceedances in Tehran are due to the given synoptic systems (Khansalari et al., 2020). On the other hand, it is technically hard to downscale and use synoptic systems as a predictor for our ANN

model. Therefore, since synoptic systems are projected in GCM models (Gibson et al., 2016), after downscaling temperature and solar radiation from GCMs by LARS-WG, these patterns are inherently included in temperature and solar radiation as dependent variables of those synoptic systems. Then, when we train our ANN model with the downscaled temperature and solar radiation as inputs to our ANN model, we inherently include some dependent variables of those synoptic systems in our trained model.

#### 2-4-1. Diurnal patterns of future temperature

Estimating the diurnal patterns of temperature for future periods can be performed using mathematical modeling. This is important in assessing the impact of climate change on peak ozone concentration levels (Millstein and Harley, 2009). In our work, to model future hourly temperatures, the diurnal pattern of future temperature was modeled by developing a mathematical model including a sinusoidal equation as a function of the time of the day (Ephrath et al., 1996):

$$T_a = T_{min} + (T_{max} - T_{min}) * S_t \quad (1)$$

where  $T_a$  is the air temperature during daytime,  $T_{min}$  and  $T_{max}$  are the minimum and maximum air temperature respectively, and  $S_t$  is a function of time  $t$ , ranging between 0 and 1, which is defined as:

$$S_t = \sin\left(\pi \frac{t - LSH + \frac{DL}{2}}{DL + 2P}\right) \quad (2)$$

where  $DL$  is the day length,  $LSH$  is the local time of maximum solar height during the day and  $P$  is the delay in the maximum air temperature concerning the time of maximum solar height at the site.

To estimate the air temperature at night, a declining exponential equation was used (Ephrath et al., 1996):

$$T_a = A + B \exp\left(-\frac{t}{\tau}\right) \quad (3)$$

which was developed to

$$T_a = \frac{T_{min(J+1)} - T_s \exp\left(-\frac{\alpha}{\tau} + (T_s - T_{min}(J+1))\right) \exp\left(\frac{t - t_s}{\tau}\right)}{1 - \exp\left(-\frac{\alpha}{\tau}\right)} \quad (4)$$

where  $\tau$  is a time coefficient considered 4;  $t_s$  and  $t_a$  are the time of sunset and the current time, respectively, and  $\alpha$  is the night length ( $\alpha = 24 - DL$ ). Values of  $DL$ ,  $LSH$  and  $P$  were extracted from temperature and solar radiation graphs, which were obtained by studying the variability of parameters during the observation period in the station under study. After inserting these parameters in the equations and by using the daily minimum and maximum temperature from LARS-WG outputs, hourly temperature values were calculated.

#### 2-4-2. Diurnal patterns of future radiation

LARS-WG generates its solar radiation output in  $Mj/m^2.day$  as the total daily radiation received by the earth's surface in a single day. However, the AQFM accepts hourly values in  $W/m^2$  as its radiation input. To match the scale of LARS-WG radiation output to the scale of the inputs to the air quality model, some equations were developed to estimate the diurnal patterns of solar radiation. The diurnal radiation curve was calculated by obtaining parameters such as daily total radiation ( $R_g$ ), day length ( $DL$ ) and solar elevation ( $\sin\beta$ ), computed from the latitude of the site ( $L$ , radians), the solar declination angle ( $\delta$ , radians) and time of the day ( $t_a$ ). To compute the sine of the solar elevation ( $\sin\beta$ ), some intermediate parameters were needed:  $SD$ , the seasonal offset of the sine of the solar height

$$SD = \sin(L) * \sin(\delta) \quad (5)$$

and  $CD$ , the amplitude of the sine of the solar height

$$CD = \cos(L) * \cos(\delta) \quad (6)$$

The sine of the solar elevation,  $\sin\beta$ , is calculated as:

$$\sin\beta = SD + CD * \cos\left(\pi \frac{t_a - LSH}{12}\right) \quad (7)$$

where  $t_a$  is the current time and  $LSH$  is the time of the maximum solar height. Instantaneous radiation ( $R_g$ ) is computed as:

$$R_g = R_g(tot) * \sin\beta * \frac{1 + C * \sin\beta}{DSBE * 3600} \quad (8)$$

where  $DSBE$  is the daily integral of  $\sin\beta(1 + \sin\beta)$  from sunrise to sunset,

calculated as:

$$DSBE = \arccos\left(-\frac{SD}{CD}\right) \frac{24}{\pi} (SD + C * SD^2 + \frac{C * CD^2}{2}) + 12 * CD * (2 + 3C * SD) * \frac{\sqrt{1 - \frac{SD^2}{CD}}}{\pi} \quad (9)$$

The parameter  $C$  (Equations (8) and (9)) is a constant meteorological variable and is considered equal to 0.4 (Spitters et al., 1986). To calculate  $SD$  and  $CD$ , a parameter called  $\delta$  is used to represent the solar declination angle. For obtaining hourly values of solar declination angle, proposed equations by Jacobson (2005) were used:

$$\delta = \arcsin(\sin \varepsilon_{ob} * \sin \lambda_{ec}) \quad (10)$$

where  $\lambda_{ec}$  represents the ecliptic longitude of the Sun and  $\varepsilon_{ob}$  represents the obliquity of the ecliptic. The ecliptic is the mean plane of the orbit of the Earth when it moves around the Sun. The obliquity of the ecliptic represents the angle between the plane of the Earth's Equator and the plane of the ecliptic, which is approximated as:

$$\varepsilon_{ob} = 23^\circ.439 - 0^\circ.0000004N_{JD} \quad (11)$$

where

$$N_{JD} = 364.5 + (Y - 2001) * 365 + D_L + D_J \quad (12)$$

$$D_L = \left\{ \left\lfloor \frac{(Y-2001)}{4} \right\rfloor \quad Y \geq 2001 \text{ or } \left\lfloor \frac{(Y-2000)}{4} \right\rfloor - 1 \right\} \quad Y < 2001 \quad (13)$$

where  $N_{JD}$  represents the number of days from the beginning of Julian year 2000. In Equations (12) and (13),  $Y$  is the current year,  $D_L$  is the number of leap days since or before the year 2000, and  $D_J$  is the Julian day of the year, which varies from 1 on 1<sup>st</sup> of January to 365 (for non-leap years) or 366 (for leap years) on 31<sup>st</sup> of December. Leap years occur every year evenly divisible by 4. The ecliptic longitude of the Sun is approximately:

$$\lambda_{ec} = L_M + 1^\circ.915 \sin(g_M) + 0^\circ.020 \sin(2g_M) \quad (14)$$

where

$$L_M = 280^\circ.460 + 0^\circ.9856474N_{JD} \quad (15)$$

$$g_M = 357^\circ.528 + 0^\circ.9856003N_{JD} \quad (16)$$

$L_M$  and  $g_M$  are the mean longitude of the Sun and the mean anomaly of the Sun,

respectively. The mean anomaly of the Sun is the angular distance, as seen by the Sun, of the Earth from its perihelion, which is the point in the Earth's orbit at which the Earth is closest to the Sun by assuming that the Earth's orbit is perfectly circular, and the Earth is moving at a constant speed.

## 2-5. Development of input scenarios to the AQFM

Estimating the future ozone concentrations under climate change required estimating the future pollution emissions together with climate conditions for the desired periods. These combinations served as inputs to our AQFM (ANN). Therefore, a combination of some pollution and climate conditions was developed as input scenarios to the AQFM to represent some probable future conditions.

### 2-5-1. Air quality scenarios

Estimating future ozone air quality conditions involve several assumptions and uncertainties (Ebi and McGregor, 2008). Future ozone production depends on emissions of its future biogenic and anthropogenic precursors such as  $NO_x$  and VOCs. Estimating future emissions of these precursors depends on key factors such as population growth, energy consumption, technological advancement, and socio-economic developments, which further involves considering limitations and uncertainties for the distant future (Webster et al., 2002). In this study, the AQFM (ANN) was trained by hourly data. Due to present limitations and uncertainties, we decided to limit our study to only the impact of climate change alone on future ozone air quality. Therefore, current pollution conditions were assumed to remain constant in the future based on hourly  $NO$  and  $NO_2$  concentrations in the summers of 2010 and 2012, which were considered pessimistic and optimistic ozone pollution scenarios, respectively. Furthermore, the main goal of this study was to get a general outlook of the future impact of climate change on future ozone extreme levels, so any year with high ozone pollution levels would be suitable for our purpose. Therefore, we selected data from two years from Golbarg air quality station as an example of upper and lower limits in ozone pollution data and as

our optimistic and pessimistic ozone pollution scenario so that the ANN model can see these example data in its training procedure. Then we trained our model with these pessimistic (high-2010) and optimistic (low-2012) ozone pollution scenarios to represent levels of ozone pollution in the historical period.

**2-5-2. Climate change scenarios**

Based on considered assumptions and limitations in the previous section we limited our study only to the effect of climate change on current pollution conditions. In this study, we used three IPCC greenhouse gas emission scenarios to simulate future climate: A1B, A2 and B1, the emissions of which are equivalent to IPCC’s Representative Concentration Pathway (RCP) greenhouse gas concentration trajectory scenarios, namely RCP4.5, RCP8.5 and RCP2.6, respectively. In this study, climate projections from HadCM3 AOGCM were used. This GCM is a coupled atmospheric-oceanic model, which has been used and suggested in several previous studies (Hessami et al., 2008; Holloway et al., 2008; Lioubimtseva and Henebry, 2009; Zarghami et al., 2011). This model simulates the global climate with 19 levels in its atmospheric component with a horizontal resolution of 2.5° by 3.75° degrees (latitude by longitude) and 20 levels in its oceanic component with a horizontal resolution of 1.25° by 1.25° degrees.

**3. Results and discussion**

**3-1. Verification of LARS-WG**

To verify the downscaled results, the ability of LARS-WG to simulate the baseline climate (1972–2009) was evaluated by coefficient of determination ( $R^2$ ), statistical tests such as t-test and K-S test, and statistical parameters such as RMSE, MAE and MBE. Table 1 indicates the calculated statistical parameters for the simulated monthly means of the climatic variables by LARS-WG in the baseline period. Except for precipitation, which has the highest simulation error, other error indices are relatively low for all variables which demonstrates the acceptable agreement between the observed and simulated monthly means in the baseline period in the study area.

**3-2. Regional changes in climate**

Figure 1 illustrates the HadCM3 projected absolute changes in surface minimum and maximum temperature for Dushan Tappeh station under A2, A1B and B1 emission scenarios. Projections were obtained for the future periods of 2015–2039 (short-term) and 2040–2064 (mid-term) relative to the baseline period (1972–2009). Long-term monthly means of observed minimum and maximum temperatures in the baseline period are also illustrated in this figure to provide an estimate of the future annual temperature patterns in the study area under climate change.

**Table 1.** Calculated statistical parameters for the simulated monthly means of the variables by LARS-WG in the baseline period at the Dushan Tappeh station (1972–2009).

Climatic variables	Error Indices		
	MBE	MAE	RMSE
Minimum Temperature	-0.03	0.12	0.15
Maximum Temperature	0.08	0.19	0.23
Solar Radiation	0.12	0.28	0.33
Precipitation	2.9	20.2	24.5

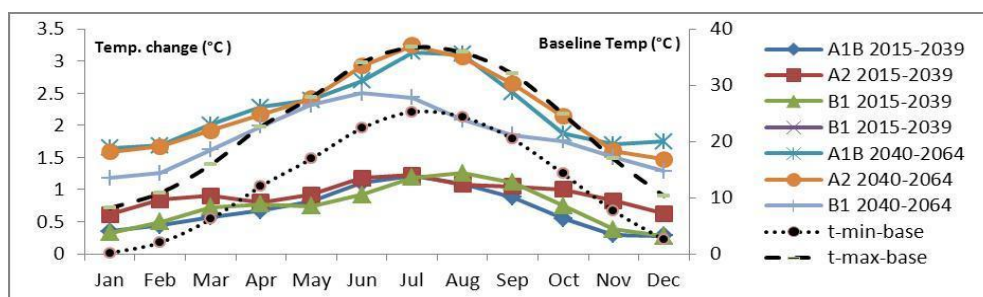


**Figure 1.** The HadCM3 projected changes in minimum (T-min) and maximum (T-max) temperature for Tehran for the short-term (2015–2039) and mid-term (2040–2064) periods concerning the baseline (1972–2009).

HadCM3 projections indicate that the monthly mean surface temperatures are expected to increase under climate change in the study area. Projections show higher average surface temperatures for all months of the year, but the increase is not uniform throughout the year. Temperature rise is projected to be higher in the warm months (JJA), which is an indication of hotter summers in the future. The average surface temperature of the study area is projected to increase by approximately 0.75 °C in the short-term and about 2.5 °C in the middle of this century. This temperature rise is expected to exceed 1 °C and 3 °C in the warm month of the year in the short-term and mid-term periods, respectively. This trend is noticeable in both short-term and mid-term climate periods. In the mid-term period changes in the projections become more distinctive among emission scenarios. Projected changes under A2 and then A1B emission scenarios are expected to be greater than changes under the B1 scenario, especially in summers where the difference is about 0.5 °C.

Figure 2 shows the projected relative changes in precipitation and radiation for the 2015–2039 and 2040–2064 climate periods concerning the baseline period under the three emission scenarios at Dushan Tappeh station. Projections illustrate explicit reverse variations in annual patterns of precipitation

and radiation under climate change in the future. Projections show that precipitation will decrease in springs and summers, while it will increase in falls and winters concerning its baseline values. Radiation, in contrast to the precipitation, is projected to increase in springs and summers, and decrease in falls and winters concerning its baseline values. The results suggest that a maximum decrease in precipitation is expected in summers, about 15% and 30% concerning the baseline period in short term and mid-term, respectively. Unlike the precipitation, the greatest increase in solar radiation is projected in summers, about 1% and 2% in short term and mid-term, respectively. These reverse patterns suggest that the decrease in precipitation and cloud cover in summers affects the amount of solar radiation received by the earth's surface in the study area. Climate simulations for future periods over the study area exhibit behaviors favorable to surface ozone formation. In general, HadCM3 GCM model projections show an increase in temperature with the greatest changes in summers under all three emission scenarios. Moreover, solar radiation is projected to increase in summers in all simulations, due to the decreases in precipitation and cloud cover over the study area. These patterns expect to influence ozone production over the study area in the future.

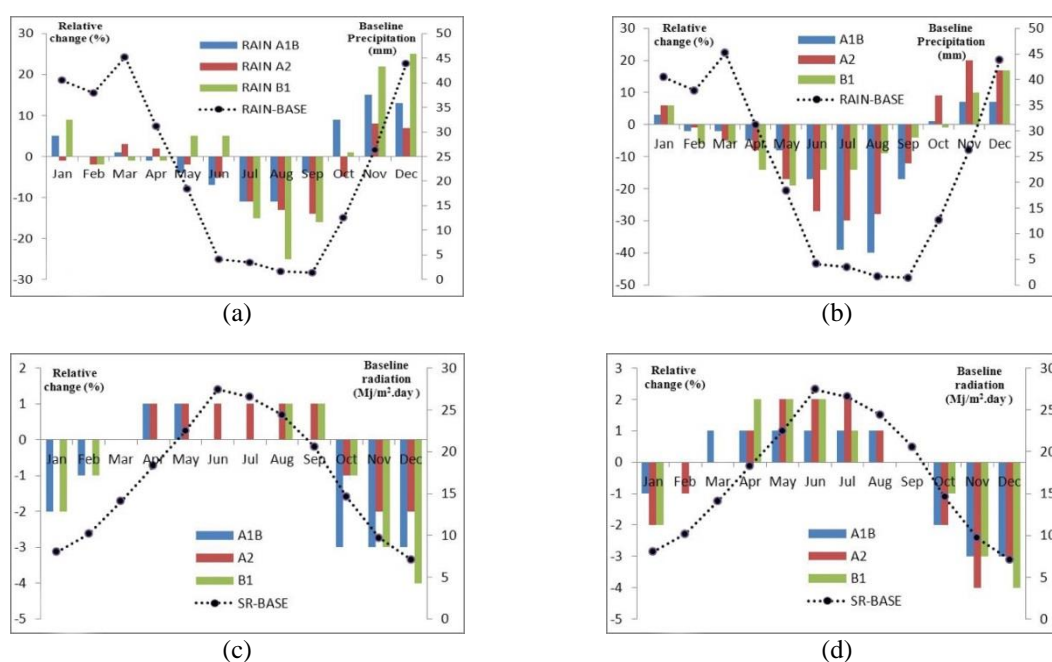


**Figure 2.** The projected relative changes in precipitation (a and b) and solar radiation (c and d) at Dushan Tappeh station for the short term (2015–2039) (left) and mid-term (2040–2064) (right).

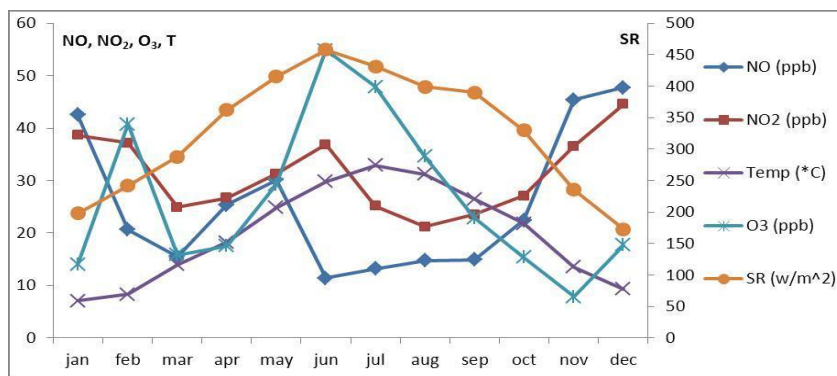
**3-3. Statistics of air quality levels in the study area**

Figure 3 illustrates the observed monthly means of the air quality variables used in this study that are averaged over the 2009–2012 period. The mean monthly variations of temperature and solar radiation indicate that the solar radiation in June, and after a month delay, the temperature in July reached their highest values. Therefore, having the highest temperatures and relatively the highest radiation, June, July and August were considered the warm months of the study area.

Moreover, Figure 3 indicates that the observed monthly mean ozone concentrations at the Golbarg air quality station have their highest values in the warm months of JJA. Ozone production in the atmosphere is highly dependent on high temperatures, which usually occur in the warm months with abundant solar radiation. Also, considering the climate projections over the study area indicate that temperature and radiation will be higher in the warm months in the future, we decided to limit the evaluation of climate change impacts on future ozone concentrations to only the warm months in

the study area, i.e., JJA.

Figure 4 clearly shows the difference between the pollution conditions in the two summers of 2010 (a) and 2012 (b) in the context of the mean diurnal variations of the variables in the JJA at the Golbarg air quality station. Among the four summers of 2009 to 2012, the summers of 2010 and 2012 had the most and the least number of days with exceedance of ozone air quality standards, respectively. The number of exceedance days was much higher in 2010 than in 2012 due to the more favorable meteorological conditions in the summer of 2010, in which, in terms of the one-hour (1-hr) ozone standard, a total of 22 days and in terms of the eight-hour (8-hr) ozone standard, a total of 58 days exceeded the 120 and 75 ppb concentration threshold, respectively. However, in the summer of 2012, no polluted day occurred in terms of any ozone air quality standard. Table 2 also shows the statistical characteristics of the variables for the two summers. The summer of 2010 experienced higher ozone concentrations in JJAs compared to the summer of 2012 in terms of both seasonal means and mean diurnal concentrations.



**Figure 3.** Mean annual cycles of NO, NO<sub>2</sub>, ozone (O<sub>3</sub>), solar radiation (SR) and temperature (T) at the Golbarg air quality monitoring station for the period 2009–2012.

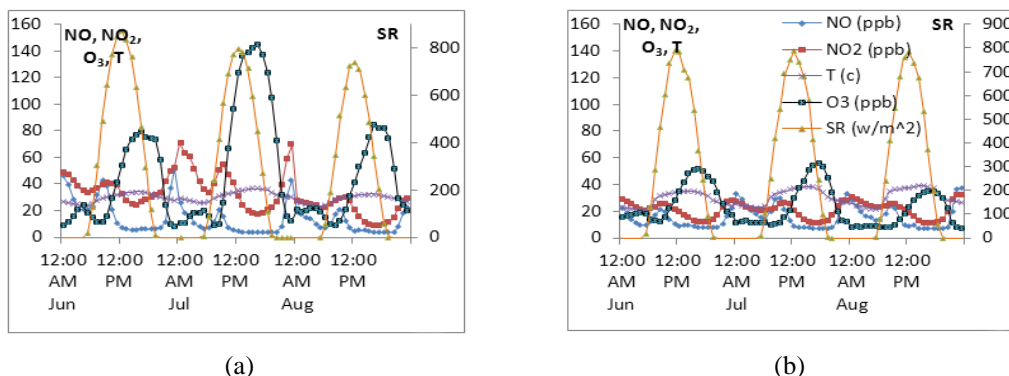


**Figure 4.** Mean diurnal cycles of nitrogen monoxide (NO), nitrogen dioxide (NO<sub>2</sub>), ozone (O<sub>3</sub>), solar radiation (SR) and temperature (T) at the Golbarg air quality monitoring station for the summers of 2010 (a) and 2012 (b).

**Table 2.** Statistical review of the pollution and meteorological variables for the summers of 2010 and 2012. Variables are like those in Figure 4.

Summer 2010	Variables	Minimum	Maximum	Average	Standard deviation
	NO (ppb)	3.5	106	9.3	13.9
	NO <sub>2</sub> (ppb)	4	149	26.6	17
	ozone (ppb)	4	280.4	71.2	51.8
	T (°C)	23.58	42.67	32.6	3.1
	SR (w/m <sup>2</sup> )	0	939	506.1	270.3
	Summer 2012	Variables	Minimum	Maximum	Average
NO (ppb)		6.5	82.14	11.7	9.8
NO <sub>2</sub> (ppb)		7.2	50.17	17.5	7.26
ozone (ppb)		6.5	96.53	33.45	17.56
T (°C)		20.54	43.1	35	3.66
SR (w/m <sup>2</sup> )		0	902	493	272.3

### 3-4. Development and validation of the AQFM

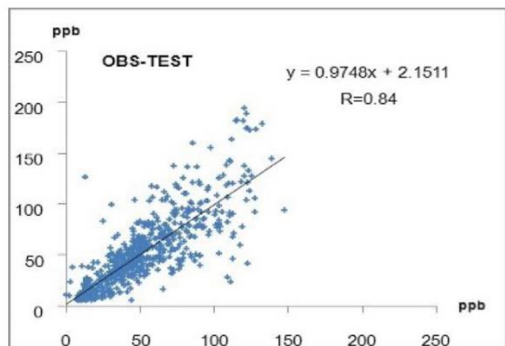
To find the optimal architecture for the AQFM, several structures with different numbers of hidden layers and nodes were evaluated. Two out of several various examined architectures with the calculated statistical parameters from the test data sets are shown in Table 3. Statistical parameters indicate that the network with two hidden layers, which has a higher correlation coefficient (R) and lower MBE, MAE and RMSE, can better capture the complex and nonlinear relationships among variables of the model. Consequently, the architecture with two hidden layers was selected for the AQFM.

Figure 5 shows the scatter plot of simulated and observed ozone concentrations for the test data set, illustrates the degree of correlation between the two variables, and presents the corresponding correlation

coefficient on the plot. The correlation coefficient is 0.84, which indicates an acceptable agreement between observed and simulated ozone concentrations at the Golbarg air quality monitoring station. The MBE index is about  $-0.9$  ppb. The negative value indicates that the forecast model underestimates the hourly ozone concentrations about 0.9 ppb under the actual observed values. This can be due to the absence of VOC concentrations in the simulation process (Liu et al., 1987). The evaluation criteria of the forecast model are in the acceptable range compared to other similar studies (Arhami et al., 2013; Comrie, 1997; Sousa et al., 2007). In comparison with similar studies, the MAE and RMSE, about 13.8 and 20.43 ppb, respectively, are also in the acceptable range that indicates the acceptable performance of the AQFM in predicting hourly ozone concentrations with the least number of input variables.

**Table 3.** Calculated statistical parameters for our two developed models.

	No. of neurons	R	MBE	MAE	RMSE
1 hidden layer	10	0.82	-1.77	14.5	21.38
2 hidden layers	10	0.84	-0.9	13.8	20.43



**Figure 5.** Scatter plot illustrating the correlation between simulated (horizontal axis) and observed ozone concentrations (vertical axis) for the test data set, together with the correlation coefficient.

Table 4 shows the ability of the AQFM to capture the exceedances of selected concentration thresholds with their corresponding references. As this table indicates, the developed model gives an acceptable prediction performance compared to a similar study (Nunnari et al., 1998). In detecting exceedances of 25 ppb and 45 ppb thresholds, the model can identify 95.7% and 85.9% of exceedances with the overestimation error of 19% and 15.7%, respectively. Moreover, in higher concentrations (exceedances of 120 ppb) the developed model can detect about 40% of exceedances with an overestimation error of about 1%. Therefore, regarding the high concentration thresholds and the number of model inputs, the AQFM represents a relatively acceptable performance in predicting the violations.

**3-5. Extracting necessary parameters for future diurnal patterns of temperature and radiation**

In the methodology section, some equations were developed to estimate the diurnal distribution of temperature in the study area. To develop these sets of equations, *DL*, *LSH* and *P* parameters were needed. We extracted these parameters from Figure 4 at the

*Golbarg* air quality station. *LSH*, the maximum solar height, was set to 12 according to Figure 4. The time lag between the occurrence of maximum temperature and maximum solar height in a day, *P*, was set to 3.5 hours according to Figure 4. The day length, *DL*, was obtained from the U.S. Navy website (<http://www.us.navy.com>) according to the location of the station and the study period. To obtain hourly temperature values during the day, the parameters were replaced in the developed temperature equations. Then, the downscaled minimum and maximum temperatures from LARS-WG for each day were replaced in the equations and hourly temperatures were obtained for each day. Solar radiation output from LARS-WG represents the daily total radiation received by the earth's surface in *Mj/m<sup>2</sup>.day*. Downscaled radiation values were distributed during the day according to the discussed approach in methodology to obtain hourly values in *w/m<sup>2</sup>*. In these sets of equations, *LSH* was considered 12 for the *Golbarg* air quality station in the study area.

**3-6. Climate change impacts on Ozone air quality**

In this study, we investigated the impact of climate change on future ozone concentrations. We investigated A1B (moderate), A2 (warm), and B1 (cool) SRES emission scenarios, and summers of 2010 and 2012 as two pollution scenarios. The pollution scenarios were considered constant based on current conditions, and therefore, only the impact of climate change on future ozone air quality was investigated by assuming that NO and NO<sub>2</sub> levels stay constant based on hourly monitored concentrations in the summers of 2010 and 2012. Finally, six different input scenarios to the AQFM were obtained and analyzed for the climate periods of 2015–2039 (short-term) and 2040–2064 (mid-term).

**Table 4.** Performance of the forecast model at selected concentration thresholds with their corresponding references (results from a similar study are shown in parentheses).

Reference	Time period	ozone threshold (ppb)	PI 1 (%)	PI 2 (%)
Ozone Standard	1 hr	125	13.8	0.48
Ozone AQI	1 hr	120	39.4	0.9
Ozone Information Level (EPA)	1 hr	90	54.5	5.4
Nunnari et al. (1998)	1 hr	45	85.9 (64.57)	15.7 (4.25)
		25	95.7 (97.75)	19 (18.03)

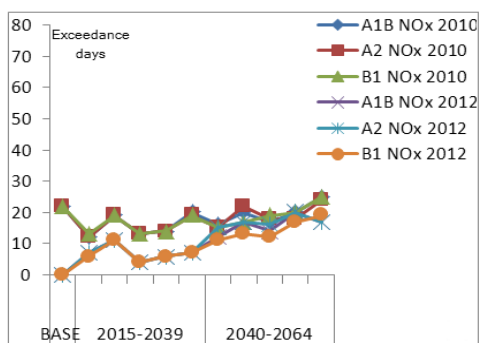
### 3-6-1. Projected trends in future ozone exceedance days

The USEPA considers the 120 and 75 ppb ozone concentrations as the thresholds for violating 1-hr and 8-hr ozone air quality standards, respectively. In this study, we used the number of days that hourly ozone concentrations exceeded each of these thresholds, so multiple exceedances within a single day were not counted for the study area.

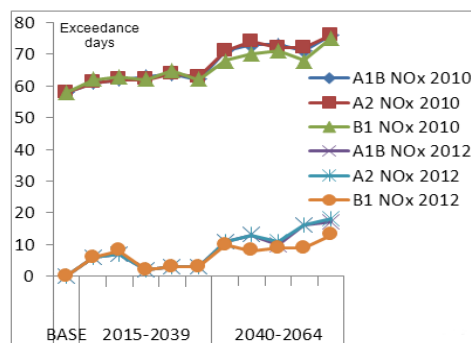
Figure 6a compares the changes in the number of days that exceed the 1-hr ozone standard in both present pollution conditions (2010 and 2012). In the summer of 2010, 22 days exceeded the 1-hr ozone standard, and no exceedances occurred in the summer of 2012. The projections indicate that the number of polluted days will increase under future climate in both emission scenarios. The number of polluted days in terms of the number of exceedances from the 1-hr standard is projected to grow, even based on the violation-free summer of 2012. Figure 6b compares the changes in the number of days that exceed the 8-hr ozone standard in both emission scenarios because of changes in future climate. Similar to 1-hr exceedances (Figure 6a), the projections show an increase in the number of 8-hr exceedances under the future climate by assuming no changes in the present pollution conditions. Although the summer of 2010 was highly polluted, climate change still has an increasing influence on the number of projected polluted days. In the mid-term, due to projected higher ozone concentrations, exceedances of the 8-hr standard will increase, and the controlling

standard will shift from 1-hr to 8-hr standard. Regardless of existing uncertainties in different parts of the climate change impact assessment such as uncertainties in climate sensitivity and future greenhouse gases emission pathways, projections indicate that because of occurring more favorable ozone formation conditions in the future due to the climate change, the number of ozone polluted days will increase overall emission scenarios and climate periods, even based on the violation-free pollution scenario of the summer of 2012. The summer of 2010 was a year with the highest monitored ozone concentrations in the observations probably due to meteorological conditions favorable to ozone formation. About 58 out of 92 days of the 2010 summer violated the 8-hr ozone standard while 2012 experienced a violation-free summer. These two scenarios can serve as a suitable example for analyzing the sensitivity of ozone air quality under future climate changes while emissions are held constant over future decades.

Furthermore, comparing changes in the projected ozone exceedances in the two climate periods, short-term changes based on each pollution scenario are almost overlapped, and no noticeable distinction exists among different emission scenarios. However, due to the inertia in the climate system, inter-scenario differences among SRES emission scenarios will emerge after 2030 and the differences among projections are more pronounced in mid-term and long-term projections (Stott and Kettleborough, 2002).



(a)



(b)

**Figure 6.** Projected days per summer (JJA) with exceedances of 1-hr (a) and 8-hr (b) ozone standard based on summers of 2010 and 2012 scenarios.

**3-6-2. The projected average number of ozone polluted days in each climate period**

Due to the stochastic nature of the downscaling techniques, it is more reasonable to consider only the changes in the number of exceedances in each climate period instead of a specific year in the future. Figure 7 illustrates the projected average number of exceedances of the 8-hr ozone standard in each climate period for each emission scenario. The number of polluted days in both emission scenarios rises in the future. In the short term, the largest increase in the number of polluted days is anticipated for the B1 emission scenario and in the mid-term, the largest increase is projected for the A2 simulations. In the short term and based on the summer of 2010 scenario, the largest increase is expected to be about 8.3% for the B1 scenario from 58 exceedance days in 2010 to 62.8 exceedance days in the short term. In the mid-term, the largest increase is expected to be about 26% for the A2 scenario from 58 exceedance days in 2010 to 73 exceedance days in the mid-term. Likewise, based on the summer of 2012 scenario, all scenarios show an increase in the number of

exceedance days. In the short term, the largest increase in the number of exceedance days is anticipated for the B1 scenario, and this number grows from zero in 2012 to 4.4 days in the short term. In the mid-term, the largest increase in the number of exceedance days is projected for the A2 scenario, and this number grows from zero in 2012 to 13.8 days in the mid-term.

**3-6-3. Projected trends in future ozone Air Quality Index exceedances (AQI)**

The projected ozone concentrations were also analyzed from health-related metrics such as 1-hr and 8-hr ozone Air Quality Indices (AQI). In this section, only the 8-hr projections for the A1B emission scenario are presented. Figure 8 shows the change in the number of days with exceedance of the 8-hr ozone AQI concentration thresholds under the A1B emission scenario for the summers of 2010 (a) and 2012 (b). Projections indicate an increase in the number of ozone *Unhealthy* and *Very Unhealthy* days under the impact of climate change, which reflects the degradation of ozone air quality in the future.

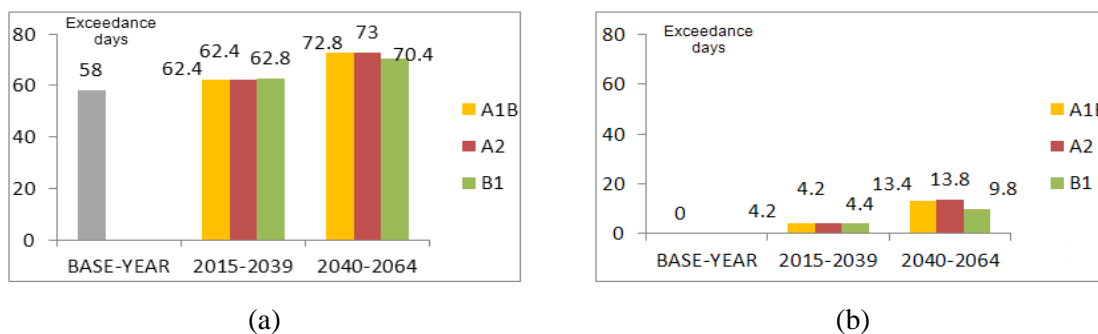


**Figure 7.** The projected average number of summer days (JJA) with exceedance of 8-hr ozone standard based on summers of 2010 (a) and 2012 (b).

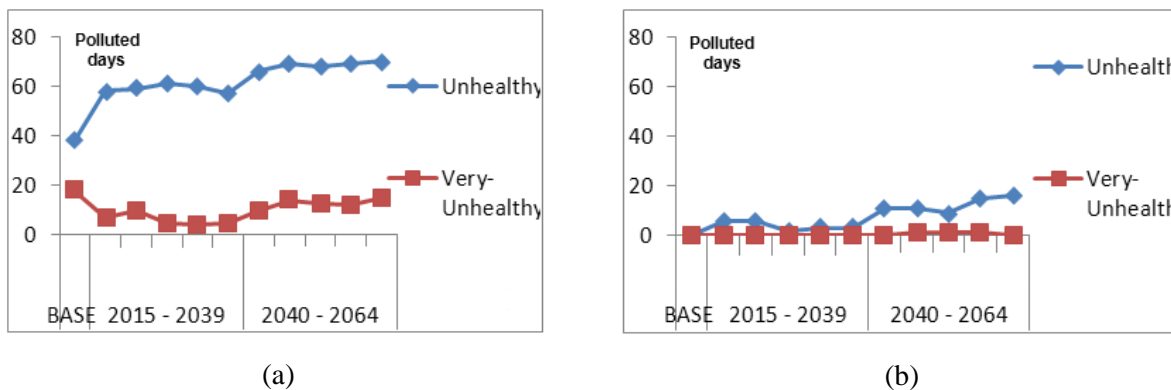


**Figure 8.** The projected days per summer (JJA) with exceedances of 8-hr ozone AQI based on summers of 2010 (a) and 2012 (b).

Figure 8a shows that based on the summer of 2010 scenario, the number of *Unhealthy* days increases over both climate periods, while the number of *Very Unhealthy* days decreases over the first period and then increases in the second period. Figure 8b shows that based on the summer 2010 scenario, the number of *Unhealthy* days grows over the two future climate periods. The occurrence of *Very Unhealthy* days is not expected over the first climate period, but due to the projected higher temperature and radiation, the number of *Very Unhealthy* days starts to grow over the second climate period.

The average number of polluted days was calculated for each climate period. In this section, only the projections for the 8-hr ozone AQI under the A1B emission scenario are demonstrated. Figure 9 shows the average number of polluted days in the 8-hr ozone AQI for the pollution conditions in the summers of 2010 (a) and 2012 (b). As Figure 9a shows, the average number of *Unhealthy* days is expected to grow over the two future climate periods. The number of *Unhealthy* days was 38 days in the summer of 2010, which is projected to increase by about 55% over the first period, averaging about 59 days in the short term, and about 80% over the second period, averaging about 68.5 days in the mid-term. The number of *Very Unhealthy* days is projected to fall about 65% from 18 days in the summer of 2010 to 6.2 days in the first period but is projected to double in the second period by increasing from 6.2 days to 12.8 days in the mid-term period.

Figure 9b shows an increase in the average number of polluted days based on the summer 2012 scenario. No *Unhealthy* day was observed in the summer 2012. However, projections estimate about 4 *Unhealthy* days without any *Very Unhealthy* days in the short-term period. In the mid-term period, the average number of *Unhealthy* days is expected to increase to 12 days with one *Very Unhealthy* day.

#### 4. Summary and conclusion

In this study, we investigated the impact of climate change on future summer ozone concentrations in Tehran, Iran. We used three

IPCC greenhouse gas emission scenarios to simulate future climate: A1B, A2 and B1, the emissions of which are equivalent to RCP4.5, RCP8.5 and RCP2.6, respectively. These climate projections were obtained from HACM3 GCM and were downscaled by the LARS-WG5 model over the periods of 2015–2039 and 2040–2064. The main goal of this study was to get a general outlook of ozone levels in the future impacted by climate change. A model trained with average ozone levels can only simulate average exceedances, but we wanted to include extreme pollution exceedances in our training data and simulate optimistic and pessimistic scenarios in the training procedure of our ANN model. Therefore, we included the two high and low ozone levels as the upper and lower range of pollution levels in our training data.

The projected increases in temperature and solar radiation along with the decreases in precipitation and cloud cover for the future summers over the study area are indications of more favorable conditions for photochemical pollution formation, which could consequently result in degraded air quality conditions in future summers. To quantify the impact of projected climate change on future ozone levels, we developed a neural network as our AQFM. We used hourly temperature, solar radiation, NO and NO<sub>2</sub> as inputs to our AQFM. The projections were performed by assuming that the current emission conditions of ozone precursors remain constant in the future. Therefore, pollution conditions of the summers of 2010 and 2012 were considered as two different pollution scenarios, and only the impact of climate change alone was accounted for in the projections. The simulations project that the number of ozone-polluted days would increase based on both summer emission scenarios. The increase based on the exceedance-free summer 2012 would be more noticeable compared to the highly polluted summer of 2010. Moreover, the growing number of polluted days in terms of 8-hr indices compared to 1-hr indices could be an indication of more exposure to higher ozone concentrations in the future.

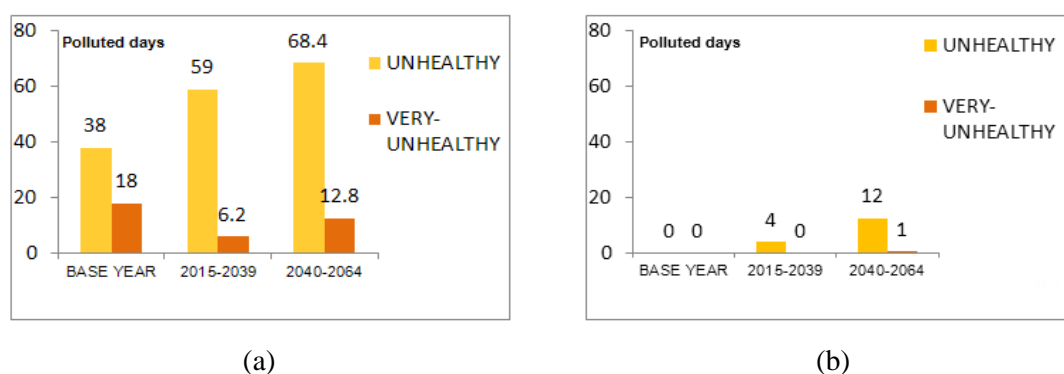


**Figure 9.** The projected average number of summer days (JJA) with exceedance of 8-hr ozone AQI based on summers 2010 (a) and 2012 (b).

Since this study is considered one of the first studies in Iran that address the influence of future climate on air quality, it was subject to various limitations. One of the major limitations was that NMVOC concentrations were not included in the simulations due to the unavailability of this data. Ozone simulations without considering NMVOCs in the calculation process tend to underestimate ozone concentrations (Liu et al., 1987). Ozone production is sensitive to other climate variables such as wind speed, water vapor, cloud cover, or precipitation (Dawson et al., 2007). However, due to the simplification in the modeling process, only temperature and solar radiation were selected in this study. Another limitation of this study is the assumption that emissions of ozone precursors and their relationship with ozone formation remain constant in the future, and therefore, the role of future emission reductions cannot be considered in the simulations. To reduce the scope of this limitation in our simulations, two different summertime pollution conditions with the highest and the lowest number of monitored polluted days were considered in this modeling endeavor to demonstrate the probable range of future changes in ozone pollution.

Future research should therefore consider the limitations of this study. Since the absence of NMVOC concentrations as one of the main precursors of ozone production reduces the accuracy of the simulations, future studies could benefit from including NMVOC concentrations in simulations. Moreover, regarding existing uncertainties in GCM projections, future studies should also consider ensemble projection approaches by

incorporating several GCMs in climate change impact assessments to improve the level of confidence in air quality projections. Furthermore, using dynamical downscaling results from Regional Climate Models (RCMs), including other climate variables in projections, and comparing projections of statistical approaches with projections of Chemistry Transport Models (CTMs) could be other useful measures to consider for improving the accuracy and confidence in the climate change impact assessments.

## References

- Alibak, A.H., Khodarahmi, M., Fayyazsanavi, P., Alizadeh, S.M., Hadi, A.J., & Aminzadehsarikhanbeglou, E. (2022). Simulation the adsorption capacity of polyvinyl alcohol/carboxymethyl cellulose based hydrogels towards methylene blue in aqueous solutions using cascade correlation neural network (CCNN) technique. *J. Clean. Prod.*, 337, 130509. <https://doi.org/10.1016/j.jclepro.2022.130509>.
- Arhami, M., Kamali, N., & Rajabi, M.M. (2013). Predicting hourly air pollutant levels using artificial neural networks coupled with uncertainty analysis by Monte Carlo simulations, *Environ. Sci. Pollut. Res.*, 20, 4777–4789. <https://doi.org/10.1007/s11356-012-1451-6>.
- Atash, F. (2007). The deterioration of urban environments in developing countries: Mitigating the air pollution crisis in Tehran, Iran. *Cities*, 24, 399–409. <https://doi.org/10.1016/j.cities.2007.04.001>.

- Beale, M.H., Hagan, M.T., & Demuth, H.B. (2012). *Neural Network Toolbox™ User's Guide*, in: R2012a, The MathWorks, Inc., 3 Apple Hill Drive Natick, MA 01760-2098, [Www.Mathworks.Com](http://www.mathworks.com).
- Bell, M.L., Goldberg, R., Hogrefe, C., Kinney, P.L., Knowlton, K., Lynn, B., Rosenthal, J., Rosenzweig, C., & Patz, J.A. (2007). Climate change, ambient ozone, and health in 50 US cities. *Clim. Change*, 82, 61–76. <https://doi.org/10.1007/s10584-006-9166-7>.
- Camalier, L., Cox, W., & Dolwick, P. (2007). The effects of meteorology on ozone in urban areas and their use in assessing ozone trends. *Atmos. Environ.*, 41, 7127–7137. <https://doi.org/10.1016/j.atmosenv.2007.04.061>.
- Chaloulakou, A., Saisana, M., & Spyrellis, N. (2003). Comparative assessment of neural networks and regression models for forecasting summertime ozone in Athens. *Sci. Total Environ.*, 313, 1–13. [https://doi.org/10.1016/S0048-9697\(03\)00335-8](https://doi.org/10.1016/S0048-9697(03)00335-8).
- Comrie, A.C. (1997). Comparing Neural Networks and Regression Models for Ozone Forecasting. *J. Air Waste Manag. Assoc.*, 47, 653–663. <https://doi.org/10.1080/10473289.1997.10463925>.
- Cox, W.M., & Chu, S. H. (1996). Assessment of interannual ozone variation in urban areas from a climatological perspective. *Atmos. Environ.*, 30, 2615–2625. [https://doi.org/10.1016/1352-2310\(95\)00346-0](https://doi.org/10.1016/1352-2310(95)00346-0).
- Dawson, J.P., Adams, P.J., & Pandis, S.N. (2007). Sensitivity of ozone to summertime climate in the eastern USA: A modeling case study. *Atmos. Environ.*, 41, 1494–1511. <https://doi.org/10.1016/j.atmosenv.2006.10.033>.
- Dawson, J.P., Racherla, P.N., Lynn, B.H., Adams, P.J., & Pandis, S.N. (2009). Impacts of climate change on regional and urban air quality in the eastern United States: Role of meteorology. *J. Geophys. Res. Atmospheres*, 114. <https://doi.org/10.1029/2008JD009849>.
- Ebi, K.L., & McGregor, G. (2008). Climate Change, Tropospheric Ozone and Particulate Matter, and Health, Impacts. *Environ. Health Perspect.*, 116, 1449–1455. <https://doi.org/10.1289/ehp.11463>.
- Ephrath, J.E., Goudriaan, J., & Marani, A. (1996). Modelling diurnal patterns of air temperature, radiation wind speed, and relative humidity by equations from daily characteristics. *Agric. Syst.*, 51, 377–393. [https://doi.org/10.1016/0308-521X\(95\)00068-G](https://doi.org/10.1016/0308-521X(95)00068-G).
- Fuentes, J.D., Lerda, M., Atkinson, R., Baldocchi, D., Bottenheim, J.W., Ciccioli, P., Lamb, B., Geron, C., Gu, L., Guenther, A., Sharkey, T.D., & Stockwell, W. (2000). Biogenic Hydrocarbons in the Atmospheric Boundary Layer: A Review. *Bull. Am. Meteorol. Soc.*, 81, 1537–1575.
- Gardner, M.W., & Dorling, S.R. (1998). Artificial neural networks (the multilayer perceptron)—a review of applications in the atmospheric sciences. *Atmos. Environ.*, 32, 2627–2636. [https://doi.org/10.1016/S1352-2310\(97\)00447-0](https://doi.org/10.1016/S1352-2310(97)00447-0).
- Gibson, P.B., Perkins-Kirkpatrick, S.E., & Renwick, J.A. (2016). Projected changes in synoptic weather patterns over New Zealand examined through self-organizing maps. *International Journal of Climatology*, 36, 3934–3948. <https://doi.org/10.1002/joc.4604>.
- Gryparis, A., Forsberg, B., Katsouyanni, K., Analitis, A., Touloumi, G., Schwartz, J., Samoli, E., Medina, S., Anderson, H.R., Niciu, E.M., Wichmann, H.-E., Kriz, B., Kosnik, M., Skorkovsky, J., Vonk, J.M., & Dörtbudak, Z. (2004). Acute Effects of Ozone on Mortality from the “Air Pollution and Health A European Approach” Project. *Am. J. Respir. Crit. Care Med.*, 170, 1080–1087. <https://doi.org/10.1164/rccm.200403-333OC>.
- Guenther, A., Geron, C., Pierce, T., Lamb, B., Harley, P., & Fall, R. (2000). Natural emissions of non-methane volatile organic compounds, carbon monoxide, and oxides of nitrogen from North America. *Atmos. Environ.*, 34, 2205–2230. [https://doi.org/10.1016/S1352-2310\(99\)00465-3](https://doi.org/10.1016/S1352-2310(99)00465-3).
- Halek, F., Kavouci, A., & Montehaie, H. (2004). Role of motor-vehicles and trend of air borne particulate in the Great

- Tehran area, Iran. *Int. J. Environ. Health Res.*, 14, 307–313. <https://doi.org/10.1080/09603120410001725649>.
- Hessami, M., Gachon, P., Ouarda, T.B.M.J., & St-Hilaire, A. (2008). Automated regression-based statistical downscaling tool. *Environ. Model. Softw.*, 23, 813–834. <https://doi.org/10.1016/j.envsoft.2007.10.004>.
- Holloway, T., Spak, S.N., Barker, D., Bretl, M., Moberg, C., Hayhoe, K., Van Dorn, J., & Wuebbles, D. (2008). Change in ozone air pollution over Chicago associated with global climate change. *J. Geophys. Res. Atmospheres*, 113. <https://doi.org/10.1029/2007JD009775>.
- Hosseinpoor, A.R., Forouzanfar, M.H., Yunesian, M., Asghari, F., Naieni, K.H., & Farhood, D. (2005). Air pollution and hospitalization due to angina pectoris in Tehran, Iran: A time-series study. *Environ. Res.*, 99, 126–131. <https://doi.org/10.1016/j.envres.2004.12.004>.
- Hoveidi, H., Aslemand, A., Vahidi, H., & Akhavan, F. (2013). Cost Emission of Pm10 on Human Health Due to the Solid Waste Disposal Scenarios, Case Study; Tehran, Iran. *J. Earth Sci. Clim. Change.*, <https://doi.org/10.4172/2157-7617.1000139>.
- IPCC, (2021). Summary for Policymakers. In: Climate Change 2021: The Physical Science Basis. Contribution of Working Group I to the Sixth Assessment Report of the Intergovernmental Panel on Climate Change [Masson-Delmotte, V., P. Zhai, A. Pirani, S.L. Connors, C. Péan, S. Berger, N. Caud, Y. Chen, L. Goldfarb, M.I. Gomis, M. Huang, K. Leitzell, E. Lonnoy, J.B.R. Matthews, T.K. Maycock, T. Waterfield, O. Yelekçi, R. Yu, and B. Zhou (eds.)]. Cambridge University Press, Cambridge, United Kingdom and New York, NY, USA, pp. 3–32, doi:10.1017/9781009157896.001.
- IPCC, (2007). Summary for Policymakers. In: Climate Change 2007: The Physical Science Basis. Contribution of Working Group I to the Fourth Assessment Report of the Intergovernmental Panel on Climate Change [Solomon, S., D. Qin, M. Manning, Z. Chen, M. Marquis, K.B. Averyt, M.Tignor and H.L. Miller (eds.)]. Cambridge University Press, Cambridge, United Kingdom and New York, NY, USA.
- Jacob, D.J., & Winner, D.A. (2009). Effect of climate change on air quality. *Atmos. Environ.*, 43, 51–63. <https://doi.org/10.1016/j.atmosenv.2008.09.051>.
- Jacobson, M.Z. (2005). Fundamentals of Atmospheric Modeling, 2nd ed. Cambridge University Press, Cambridge. <https://doi.org/10.1017/CBO9781139165389>.
- Khansalari, S., Ghobadi, N., Bidokhti, A., & Fazel-Rastgar, F. (2020). Statistical classification of synoptic weather patterns associated with Tehran air pollution. *J. Air Pollut. Health*, 5, 43–62. <https://doi.org/10.18502/japh.v5i1.2858>.
- Lee, B. S., & Wang, J. L. (2006). Concentration variation of isoprene and its implications for peak ozone concentration. *Atmos. Environ.*, 40, 5486–5495. <https://doi.org/10.1016/j.atmosenv.2006.03.035>.
- Leibensperger, E.M., Mickley, L.J., & Jacob, D.J. (2008). Sensitivity of US air quality to mid-latitude cyclone frequency and implications of 1980–2006 climate change. *Atmospheric Chem. Phys.*, 8, 7075–7086. <https://doi.org/10.5194/acp-8-7075-2008>.
- Liao, H., Chen, W.-T., & Seinfeld, J.H. (2006). Role of climate change in global predictions of future tropospheric ozone and aerosols. *J. Geophys. Res. Atmospheres*, 111. <https://doi.org/10.1029/2005JD006852>.
- Lioubimtseva, E., & Henebry, G.M. (2009). Climate and environmental change in arid Central Asia: Impacts, vulnerability, and adaptations. *J. Arid Environ.*, 73, 963–977. <https://doi.org/10.1016/j.jaridenv.2009.04.022>.
- Liu, S.C., Trainer, M., Fehsenfeld, F.C., Parrish, D.D., Williams, E.J., Fahey, D.W., Hübler, G., & Murphy, P.C. (1987). Ozone production in the rural troposphere and the implications for regional and global ozone distributions. *J. Geophys. Res. Atmospheres*, 92, 4191–4207.

- <https://doi.org/10.1029/JD092iD04p04191>.
- Lynn, B.H., Druyan, L., Hogrefe, C., Dudhia, J., Rosenzweig, C., Goldberg, R., Rind, D., Healy, R., Rosenthal, J., & Kinney, P. (2004). Sensitivity of present and future surface temperatures to precipitation characteristics. *Clim. Res.*, 28, 53–65. <https://doi.org/10.3354/cr028053>.
- Mejia, J., Wilcox, E., Rayne, S., & Mosadegh, E. (2018). Final report: Vehicle Miles Traveled Review, <https://doi.org/10.13140/RG.2.2.29814.52807>.
- Millstein, D.E., & Harley, R.A. (2009). Impact of climate change on photochemical air pollution in Southern California. *Atmospheric Chem. Phys.*, 9, 3745–3754. <https://doi.org/10.5194/acp-9-3745-2009>.
- Mosadegh, E. (2013). Modeling the Regional Effects of Climate Change on Future Urban Air Quality (With Special Reference to Future Ozone Concentrations in Tehran, Iran), Univ. Tehran, Iran. DOI: 10.13140/RG.2.2.23815.32165.
- Mosadegh, E., & Babaeian, I. (2022a). Projection of Temperature and Precipitation for 2020-2100 Using Post-processing of General Circulation Models Output and Artificial Neural Network Approach, Case Study: Tehran and Alborz Provinces. *Iranian Journal of Geophysics*. <https://doi.org/10.30499/ijg.2022.311104.1370>.
- Mosadegh, E., & Babaeian, I. (2022b). Quantifying the Range of Uncertainty in GCM Projections for Future Solar Radiation, Temperature and Precipitation under Global Warming Effect in Dushan-Tappeh Station, Tehran, Iran. *Iranian Journal of Geophysics*. <https://doi.org/10.30499/ijg.2022.310958.1369>.
- Mosadegh, E., Mejia, J., Wilcox, E.M., & Rayne, S. (2018). Vehicle Miles Travel (VMT) trends over Lake Tahoe area and its effect on Nitrogen Deposition, A23M-3068.
- Mosadegh, E., & Nolin, A.W. (2020). Estimating Arctic sea ice surface roughness by using back propagation neural network, C014-0005.
- Mosadegh, E., & Nolin, A.W. (2022). A New Data Processing System for Generating Sea Ice Surface Roughness Products from the Multi-Angle Imaging SpectroRadiometer (MISR) Imagery. *Remote Sens.*, 14, 4979. <https://doi.org/10.3390/rs14194979>.
- Mott, J.A., Mannino, D.M., Alverson, C.J., Kiyu, A., Hashim, J., Lee, T., Falter, K., & Redd, S.C. (2005). Cardiorespiratory hospitalizations associated with smoke exposure during the 1997, Southeast Asian forest fires. *Int. J. Hyg. Environ. Health*, 208, 75–85. <https://doi.org/10.1016/j.ijheh.2005.01.018>.
- Murazaki, K., & Hess, P. (2006). How does climate change contribute to surface ozone change over the United States. *J. Geophys. Res. Atmospheres*, 111. <https://doi.org/10.1029/2005JD005873>.
- Narumi, D., Kondo, A., & Shimoda, Y. (2009). The effect of the increase in urban temperature on the concentration of photochemical oxidants. *Atmos. Environ.*, 43, 2348–2359. <https://doi.org/10.1016/j.atmosenv.2009.01.028>.
- Nejatishahidin, N., Fayyazsanavi, P., & Kosecka, J. (2022). Object Pose Estimation using Mid-level Visual Representations (No. arXiv:2203.01449). <https://doi.org/10.48550/arXiv.2203.01449>.
- Niska, H., Hiltunen, T., Karppinen, A., Ruuskanen, J., & Kolehmainen, M. (2004). Evolving the neural network model for forecasting air pollution time series, *Eng. Appl. Artif. Intell., Intelligent Control and Signal Processing*, 17, 159–167. <https://doi.org/10.1016/j.engappai.2004.02.002>.
- Nunnari, G., Nucifora, A.F.M., & Randieri, C. (1998). The application of neural techniques to the modelling of time-series of atmospheric pollution data. *Ecol. Model.*, 111, 187–205. [https://doi.org/10.1016/S0304-3800\(98\)00118-5](https://doi.org/10.1016/S0304-3800(98)00118-5).
- Ordóñez, C., Mathis, H., Furger, M., Henne, S., Hüglin, C., Staehelin, J., & Prévôt, A.S.H. (2005). Changes of daily surface ozone maxima in Switzerland in all

- seasons from 1992 to 2002 and discussion of summer 2003. *Atmospheric Chem. Phys.*, 5, 1187–1203. <https://doi.org/10.5194/acp-5-1187-2005>.
- Orru, H., Andersson, C., Ebi, K.L., Langner, J., Åström, C., & Forsberg, B. (2013). Impact of climate change on ozone-related mortality and morbidity in Europe. *Eur. Respir. J.*, 41, 285–294. <https://doi.org/10.1183/09031936.00210411>.
- Racherla, P.N., & Adams, P.J. (2006). Sensitivity of global tropospheric ozone and fine particulate matter concentrations to climate change. *J. Geophys. Res. Atmospheres*, 111. <https://doi.org/10.1029/2005JD006939>.
- Rahnama, M., & Noury, M. (2008). Developing of Halil River Rainfall-Runoff Model, Using Conjunction of Wavelet Transform and Artificial Neural Networks. *Res. J. Environ. Sci.*, 2, 385–392. <https://doi.org/10.3923/rjes.2008.385.392>.
- Schlink, U., Dorling, S., Pelikan, E., Nunnari, G., Cawley, G., Junninen, H., Greig, A., Foxall, R., Eben, K., Chatterton, T., Vondracek, J., Richter, M., Dostal, M., Bertuccio, L., Kolehmainen, M., & Doyle, M. (2003). A rigorous inter-comparison of ground-level ozone predictions. *Atmos. Environ.*, 37, 3237–3253. [https://doi.org/10.1016/S1352-2310\(03\)00330-3](https://doi.org/10.1016/S1352-2310(03)00330-3).
- Seinfeld, J.H., & Pandis, S.N. (2006). *Atmospheric chemistry and physics: from air pollution to climate change*, 2nd ed. Wiley, Hoboken, N.J.
- Semenov, M., & Barrow, E. (2002). LARS-WG A Stochastic Weather Generator for Use in Climate Impact Studies.
- Semenov, M., & Stratonovitch, P. (2010). Use of multi-model ensembles from global climate models for assessment of climate change impacts. *Clim. Res.*, 41, 1–14. <https://doi.org/10.3354/cr00836>.
- Semenov, M.A. (2007). Development of high-resolution UKCIP02-based climate change scenarios in the UK. *Agric. For. Meteorol.*, 144, 127–138. <https://doi.org/10.1016/j.agrformet.2007.02.003>.
- Sillman, S. (1999). The relation between ozone, NO<sub>x</sub> and hydrocarbons in urban and polluted rural environments. *Atmos. Environ.*, 33, 1821–1845. [https://doi.org/10.1016/S1352-2310\(98\)00345-8](https://doi.org/10.1016/S1352-2310(98)00345-8).
- Sillman, S., & Samson, P.J. (1995). Impact of temperature on oxidant photochemistry in urban, polluted rural and remote environments. *J. Geophys. Res. Atmospheres*, 100, 11497–11508. <https://doi.org/10.1029/94JD02146>.
- Sousa, S.I.V., Martins, F.G., Alvim-Ferraz, M.C.M., & Pereira, M.C. (2007). Multiple linear regression and artificial neural networks based on principal components to predict ozone concentrations. *Environ. Model. Softw.*, 22, 97–103. <https://doi.org/10.1016/j.envsoft.2005.12.002>.
- Spitters, C.J.T., Toussaint, H.A.J.M., & Goudriaan, J. (1986). Separating the diffuse and direct component of global radiation and its implications for modeling canopy photosynthesis Part I. Components of incoming radiation. *Agric. For. Meteorol.*, 38, 217–229. [https://doi.org/10.1016/0168-1923\(86\)90060-2](https://doi.org/10.1016/0168-1923(86)90060-2).
- Steiner, A.L., Tonse, S., Cohen, R.C., Goldstein, A.H., & Harley, R.A. (2006). Influence of future climate and emissions on regional air quality in California. *J. Geophys. Res. Atmospheres*, 111. <https://doi.org/10.1029/2005JD006935>.
- Stott, P.A., & Kettleborough, J.A. (2002). Origins and estimates of uncertainty in predictions of twenty-first century temperature rise. *Nature*, 416, 723–726. <https://doi.org/10.1038/416723a>.
- Varotsos, K.V., Tombrou, M., & Giannakopoulos, C. (2013). Statistical estimations of the number of future ozone exceedances due to climate change in Europe. *J. Geophys. Res. Atmospheres*, 118, 6080–6099. <https://doi.org/10.1002/jgrd.50451>.
- Webster, M.D., Babiker, M., Mayer, M., Reilly, J.M., Harnisch, J., Hyman, R., Sarofim, M.C., & Wang, C. (2002). Uncertainty in emissions projections for climate models. *Atmos. Environ.*, 36, 3659–3670. [https://doi.org/10.1016/S1352-2310\(02\)00245-5](https://doi.org/10.1016/S1352-2310(02)00245-5).
- Wilby, R., Charles, S., Zorita, E., Timbal, B., Whetton, P., & Mearns, L. (2004). *Guidelines For Use of Climate Scenarios*

- Developed From Statistical Downscaling Methods, Support. Mater., Intergov. Penel Clim. Change.
- Wilks, D.S., & Wilby, R.L. (1999). The weather generation game: a review of stochastic weather models. *Prog. Phys. Geogr. Earth Environ*, 23, 329–357. <https://doi.org/10.1177/030913339902300302>.
- Wise, E.K. (2009). Climate-based sensitivity of air quality to climate change scenarios for the southwestern United States. *Int. J. Climatol.*, 29, 87–97. <https://doi.org/10.1002/joc.1713>.
- Zarghami, M., Abdi, A., Babaeian, I., Hassanzadeh, Y., & Kanani, R. (2011). Impacts of climate change on runoffs in East Azerbaijan, Iran. *Glob. Planet. Change*, 78, 137–146. <https://doi.org/10.1016/j.gloplacha.2011.06.003>.